# Embodiment of an artificial limb in the mouse model

Zineb Hayatou, Hongkai Wang, Antoine Chaillet, Daniel E Shulz, Luc Estebanez

# Embodiment of an artificial limb in the mouse model

**Zineb Hayatou[1], Hongkai Wang[2], Antoine Chaillet[3], Daniel E. Shulz[1], Luc Estebanez[1,4]**

[1]Université Paris-Saclay, CNRS, Institut des Neurosciences Paris-Saclay, 91400 Saclay, France
[2]Faculty of Medicine, Dalian University of Technology, China
[3]Université Paris-Saclay, CNRS, CentraleSupélec, Laboratoire des signaux et systèmes, 91190 Gif-sur-Yvette, France.
[4]Corresponding author. Email: luc.estebanez@cnrs.fr

## Abstract

Having the ability to probe the strength of limb embodiment is a requirement to better understand body ownership disorders that are triggered both by disease and by accidental body damage. It is also an essential tool towards the development of neuro-prostheses that better integrate into the user's body representation.

One key way to probe limb embodiment is through the rubber hand illusion. Here we adapted this paradigm to the mouse forelimb, which is a relevant model for upper limb research thanks to its diverse and rich behavioural characteristics and unparalleled access to genetic and optogenetic research tools.

We exposed head-fixed mice to a visible, static 3D printed replica of their right forelimb, while their own forelimb was removed from their sight and stimulated by brush strokes in synchrony with the replica. Following these visuo-tactile stimulations, the replica was visually threatened, and we probed the mice's reaction using automated tracking of pupils and facial expression. We found that mice focused significantly more their gaze towards the forelimb replica when they received congruent tactile and visual information, compared to control conditions. This observation is consistent with the human overt response to the rubber hand illusion. In summary, these findings indicate that mice can experience forelimb embodiment, and this phenomenon can be evaluated with the method we developed.

## Introduction

When looking at our limbs and using them to interact with the world, we perceive that they are part of ourselves. This sense of embodiment can be disrupted by brain lesions leading to asomatognosia and somatoparaphrenia (Feinberg et al., 2010). In the case of amputated patients, efficient use of the prosthesis can be hampered by a lack of embodiment, thereby causing a decrease in daily prosthesis use and abandonment of the prosthetic limb (Espinosa & Nathan-Roberts, 2019; Maimon-Mor & Makin, 2020). Further, lack of embodiment of prosthetic substitutes is associated with a build-up of sensations that seems to arise from the "phantom" of the missing limb, including painful perceptions (Bekrater-Bodmann et al., 2021).

In an experimental setting, it is possible to either build or disrupt the sense of embodiment of an artificial limb by manipulating the temporal consistency of the tactile and visual feedback from a limb to the subject. This canonical multisensory strategy to manipulate embodiment has been widely used to study the sense of body ownership and embodiment (Botvinick & Cohen, 1998; Ehrsson et al., 2004). In particular, in the "rubber hand illusion" experiment, participants are placed next to a prosthetic limb that they can see, while their corresponding real hand is hidden from their view. Both the hidden real hand, and the visible artificial hand are stimulated in synchrony with a brush (Botvinick & Cohen, 1998). A large share of the subjects in these experiments report that the rubber hand they are seeing is their real hand as they embody the external object (Kalckert & Ehrsson, 2017; Reader et al., 2021). These verbal reports are consistent with overt behaviours of the subject during the experiment, and in particular with an anxiety-like reaction when the artificial hand is visibly threatened or "injured" by the experimenter. This is seen through higher skin conductance responses and reports of participants showing signs of anxiety or pain anticipation before the injury of the prosthesis (Armel & Ramachandran, 2003), as well

as increased activity in the insula and anterior cingulate cortex, regions that are associated with anxiety and interoceptive awareness (Ehrsson et al., 2007).

Building on the ability of visuo-tactile coordinated inputs to generate embodiment, it is even possible to induce the embodiment of an artificial device, including robotic human prostheses by stimulating the stump of amputees (Castro et al., 2023; Ehrsson et al., 2008; Rosén et al., 2009). This demonstrates the flexibility of this body-pairing mechanism, which may be key to embodied neuroprosthetics (Makin & Micera 2020). This however does not extend to any object, as studies show that the object being embodied needs to have the shape of a hand. When we replace the hand shaped object by a non-limb object, reports show a significantly weaker embodiment in these cases (Finotti et al., 2023; Tsakiris et al., 2010).

So far however, the physiology of this sensory-based forelimb embodiment remains unclear. This is partly due to the lack of a tractable animal model of embodiment. To address this, embodiment experiments have been carried in mice by applying tactile stimulations to a rubber tail and to the tail of the mouse then manually observing the animal's reaction to an experimenter grasping the tail after the end of the stimulations (Wada et al., 2016, 2019). These studies suggest that it is possible to study embodiment in mice. However, they focus on the embodiment of a body part that is very specific to rodents and can't be translated to humans in the context of research on prosthetic limbs.

Here, we have taken advantage of videography-based strategies to develop and validate an automated forelimb embodiment test in the mouse model. Automated face tracking of rodents has become a useful strategy to probe the internal state of the mouse. Face tracking reveals grimaces that are related to basic emotions of the mice and have been linked to different neuronal states (Dolensek et al., 2020), while pupil movements in particular has been related to many behavioural aspects such as fear learning, arousal and attempted movement (Langford et al., 2010; Meyer et al., 2020; Salay et al., 2018; Vinck et al., 2015).

In our paradigm, head-fixed mice were presented with an artificial, static replica of their right forelimb at a plausible physiological forelimb location. Meanwhile, their physiological forelimb was hidden from mouse sight, and stabilized in a posture consistent with the pose of the artificial limb. Next, during 2 minutes, we applied brush strokes in synchrony to the real and to the artificial forelimbs. Finally, we presented the artificial forelimb with a rapidly approaching object. Consistent with the human rubber hand illusion, the mice focused significantly more their gaze on the incoming — and potentially threatening — object when brush strokes were synchronous (versus asynchronous) and when the artificial forelimb looked similar to an actual limb (versus a white rectangular shape).

## Materials and Methods

All animal experiments were performed according to European and French law as well as CNRS guidelines and were approved by the French Ministry for Research (Ethical Committee 59, authorization 25932-2020060813556163v7). In order to reduce the number of mice involved in our research, we carried our experiment on EMX-Cre mice that were raised towards the maintenance of transgenic lines in the institute animal house, but were not directly used in other experiments. We could take advantage of these mice as they did not express any transgene and showed no noticeable difference in behaviour when compared to baseline C57BL/6 mice.

### Surgery

Implantation surgeries were carried under Isoflurane anaesthesia (4% for induction and 1-1.5% for maintenance). Surgeries were performed on a heated pad, while the mouse was held by a nose clamp. After an injection of lidocaine (4mg/kg) the scalp was cut and conjunctive tissue and skull were cleaned. A titanium head fixation plate was then bonded to the skull using a cyanoacrylate glue primer topped with dental cement. Finally, the mice received a subcutaneous injection of anti-inflammatory medication (Meloxicam, 1-8mg/kg) and were monitored during their recovery in a warmed cage.

### Recovery and habituation

The 10 mice that were tested (5 males, 5 females) were placed in the experimental setup for the first time after a 5-day recovery phase in their home cage. Each individual mouse was separately placed

inside a pod and head restrained. It was given water with sugar to associate habituation with a positive outcome. After an initial 10 min session with head fixation only, the next 4 sessions lasted 20 min of head fixation, coupled with a restriction of the right forelimb. The paw was restricted using a custom-made handcuff mechanism that was adjusted then secured on a dedicated, foam cushioned location on the pod (Figure 1A).

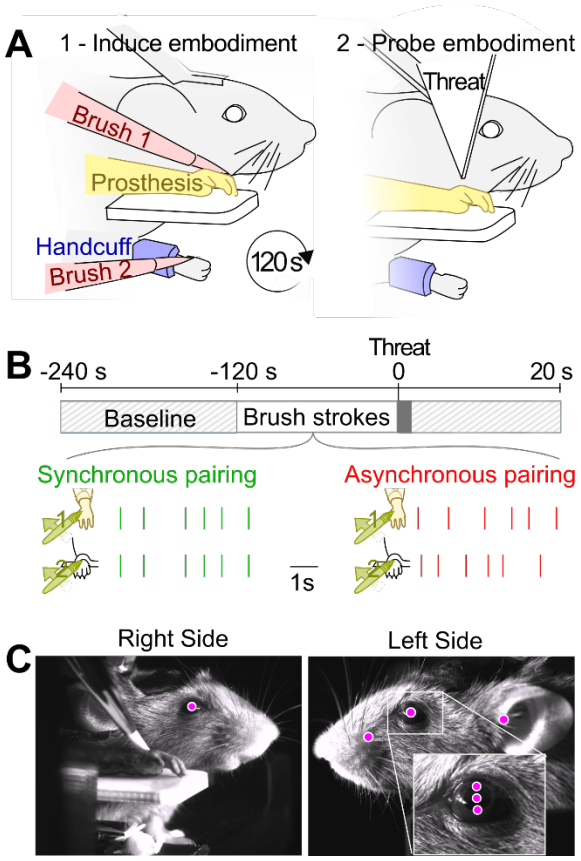


**Figure 1. A forelimb embodiment test in the mouse model.**
(**A**) Protocol schematic. During 120 seconds, brush stimulations were applied both to the artificial limb (visual input) and to the corresponding forelimb, which was hidden from the mouse's sight (touch input). Embodiment of the artificial limb was then tested by showing a rapidly incoming threat-like object that targeted the artificial limb, and by probing the intensity of the reaction of the mouse.
(**B**) Top: timeline of the pairing and test sessions. 10 mice were exposed to the protocol: 5 sessions were run for each experiment (1 session per day). During each session, the mice were exposed to 2 trials (synchronous and asynchronous). The presentation order of these two trials changed on each session. Bottom: example brush stroke times for the synchronous (green) and asynchronous (red) strokes.
(**C**) Views from the right and left side of the mouse acquired by high-speed cameras during the pairing stage. Magenta dots: points of interest that are tracked, including the pupil position and diameter (measured on 2 points in the vertical axis, see close-up) for both eyes; the left whiskerpad and ear.

### Design of the rubber hand illusion analogue

A 3D model of a right mouse forelimb was designed, based on a 3D atlas of adult C57BL/6 mice derived from micro-CT sections (Wang et al. 2015). It was printed using a resin 3D printer (FormLabs Form3B, Grey Flexible Resin) and painted using acrylic paint to match the colour of the fur of the black mice. It was placed aside the head-fixed mice, and illuminated by a ray of visible, white light (while the rest of the setup was only illuminated by infrared lighting for imaging). Meanwhile, the actual right paw of the mouse was restricted and hidden below the platform holding the artificial limb.

During the 120 s pairing time (Figure 1A left), which followed a 120 s waiting period (Figure 1B), the mouse was exposed to a series of soft strokes applied by paint brushes mounted on servo motors (Make Block Smart Servo). One "brush stroke" event was achieved by the brush making a (6 * 2 mm) back and forth movement on the paw that lasts for 300 ms between touch onset and offset (Figure 1B). During the pairing time, the brush strokes were applied both on the mouse right forelimb and on the artificial

limb, at random, Poisson-distributed intervals between 600 and 2000 ms. In the synchronous condition the two brushes apply the exact same stimulation timing, while in the asynchronous condition, each brush was activated at a different, randomized interval, such that the visual input from the artificial limb did not match the tactile input applied to the physiological forelimb (Figure 1B).

Finally, 240 s after the beginning of the trial and right after the end of the brush stimulations, a threat to the fake forelimb was presented to the mouse (Figure 1A, right). This was achieved by using a stepper motor (17HS15-0404S, OSM Technology) to rapidly move an arrow-like white plastic object towards the fake limb, at a speed of 1 degree per ms, for a total travel time of 400 ms (Figure 1C-D).

**Brush stroke pairing conditions**
The embodiment experiments using the prosthesis resembling the mice's limb lasted one week. Five sessions were run for each experiment (1 session per day). During each session, the mice were exposed to 2 trials (synchronous and asynchronous) whose order changed at each session. We chose this multi-day design to minimize mouse fatigue and reduce the effect of the habituation curve that would have been potentially more prominent if all the trials were run on the same day. 40 days later, we performed an additional, control experiment. It was identical to the initial series of pairing experiments, but this time we exposed the animals to the threat alone followed by two trials where the fake paw was replaced by a white plastic block the same size as the prosthesis (See Supplementary Table 1 for trial order).

**Face imaging and tracking**
The mice were imaged at 200Hz with two 1440x1080 px monochrome cameras capturing the right and left facial expressions (Figure 1C) using a custom high-speed imaging system (RD Vision, France). The reactions of the mice to the stimulations and the threat were recorded and the videos analysed with DeepLabCut version 2.3 (Mathis et al., 2018). We trained two networks (one network for each side of the mouse's face) on 120 labelled images of 10 different mice to track a series of points of interest on the animals face, including the center of the pupil position, 2 points of the pupil for the diameter, ear, and whiskers (magenta dots in Figure 1C)

**Statistical analysis**
To correct for baseline shifts, we subtracted the mean position of the tracked position measured during the 120 s baseline that proceeded the brush stimulations. When looking at the effect after the threat for pupil shifts and diameter, we subtracted the mean values 1s before the threat so we could normalize to pre-threat positions that may not be the same. All statistical tests were non-parametric and were Wilcoxon (paired) tests.

# Results

**Longer gaze towards the threatened prosthesis following synchronous stimulations.**
Head-fixed mice were placed on sight of a static, artificial forelimb, while their physiological right forelimb was hidden from their sight. We tracked features of their face — and in particular their pupil — during the behaviour.

During the pairing stage (Figure 1A left), both the artificial forelimb and the physiological forelimb received brush strokes, either simultaneous (synchronous stimulation), or dephased (asynchronous stimulation). At this stage, we found no significant difference in the behaviour of the mice between the synchronous and asynchronous condition, and in particular no difference in the movement of the pupils (Figure 2A-B), between the two conditions before the threat of the prosthesis (Wilcoxon test, right pupil p=0.084, Left pupil p=0.084).

After this pairing step, the artificial forelimb was almost hit by a rapidly incoming triangular object (Figure 1A, right). In both the synchronous and asynchronous pairing conditions, the mice responded to this event with a rapid pupil movement towards the artificial limb and threatening object.

One second after this first response, the mice behavior diverged between the two conditions. In the synchronous condition, on average, the mice looked again towards the menace and artificial limb, while in the asynchronous condition, the mice stopped looking in this direction and moved back their pupil

towards the resting position (Figure 2C). Overall, most of the pupil movements following the menace took place in the horizontal axis.

In particular, the pupil horizontal positions in an analysis window 2 s to 4 s after the incoming threat were significantly different in the synchronous versus asynchronous conditions, both for the right (Wilcoxon test: p=0.0098, Figure 2D and E left) and left eye (Wilcoxon test: p= 0.049, Figure 2F and G left). The same difference between synchronous and asynchronous conditions was apparent in a second time interval, 4 to 7 s after the threat was applied, for both the right (Wilcoxon test: p= 0.02, Figure 2E right) and left eye (Wilcoxon test: p= 0.049, Figure 2G right).

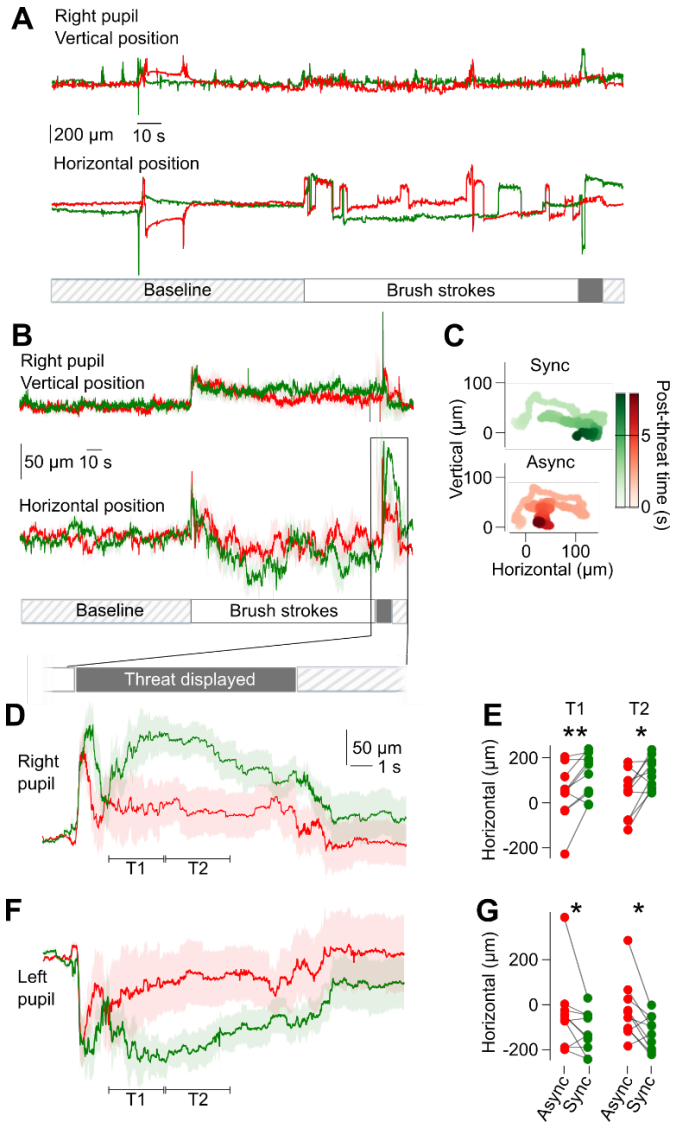


**Figure 2. Pupil shifts in the direction of the threatened prosthesis are longer after synchronous stimulation**
(**A**) Example trial of vertical (top) and horizontal (bottom) movements of the right pupil during a synchronous and an asynchronous trial (mouse 27 trial 1).
(**B**) Average vertical (top) and horizontal (bottom) movements of the right pupil during synchronous and asynchronous condition trials, normalized to the average position during the 120 s baseline (n=10). The sequence includes a Baseline, Brush strokes pairing, and a threat to the artificial forelimb (n = 10).
(**C**) Spatial distribution of the pupil position 0 to 7 s after the threat starts to be displayed. Top: synchronous pairing. Bottom: asynchronous pairing.
(**D**) Average horizontal movements of the right pupil following the threat onset, normalized relative to the average position 1 s before the threat (n=10). T1 and T2 are the time intervals tested in the Wilcoxon tests in (E). Light background: SEM
(**E**) Normalized average of right pupil positions for each mouse (n=9) during intervals T1 and T2: ****** : Wilcoxon p = 0.0098, * : Wilcoxon p = 0.02
(**F**) Same as D for the left pupil (n = 10).
(**G**) Same as E for the left pupil (n = 10). *** :** Wilcoxon p = 0.049, * : Wilcoxon p = 0.02.

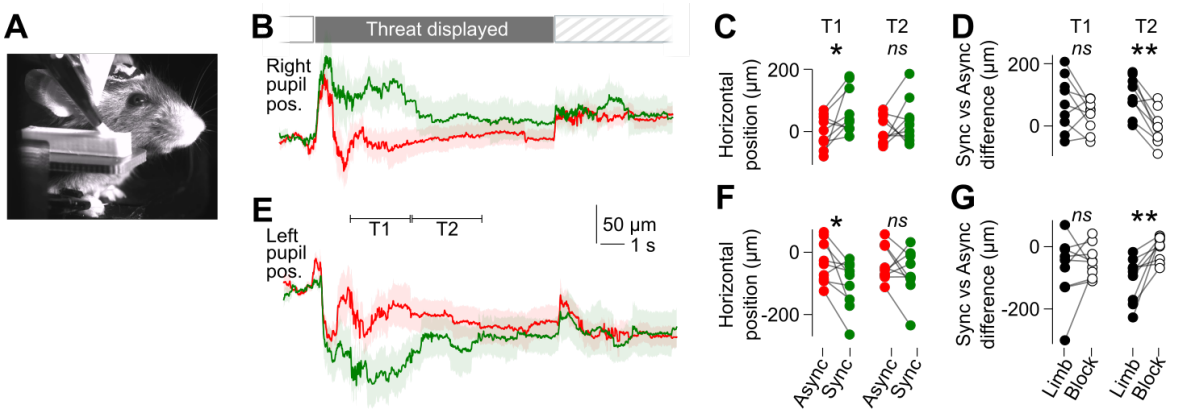


**Figure 3. Pupil shifts are shorter when the prosthesis is replaced by a white rectangle**
(**A**) Right view of the mouse and pairing setup. This time the mouse is exposed to a white rectangular object instead of the prosthesis.
(**B**) Average horizontal movements of the right pupil after the threat, normalized relative to the average position 1 s before the threat (n=9). Green line: synchronous pairing. Red: asynchronous pairing. Light background: SEM.
(**C**) Normalized average of right pupil positions for each mouse (n = 9) during the intervals T1 and T2 shown in **B**. *: Wilcoxon p = 0.039, ns: Wilcoxon p = 0.36.
(**D**) Difference between the average right pupil positions between synchronous and asynchronous conditions for the artificial limb condition (black) versus white rectangle condition (white) during intervals T1 and T2. Top: right pupil. Bottom: left pupil. ns: Wilcoxon p = 0.36, **: Wilcoxon p = 0.0039.
(**E**,**F** and **G**) same as **B**,**C** and **D** for the left pupil. **F** *: Wilcoxon p = 0.027, ns: Wilcoxon p = 0.36. **G** ns: Wilcoxon p = 0.2, **: Wilcoxon p = 0.0039.

According to human literature on the rubber hand illusion, an object that doesn't look like a hand, such as a wooden block, would show fewer signs of embodiment when compared to an artificial limb resembling a human hand (Finotti et al., 2023). We therefore hypothesized that in our experiments in the mouse model, the difference in average pupil position between synchronous and asynchronous conditions should be reduced by replacing the artificial forelimb by a non-limb object. Therefore, in a second series of experiments, we exposed our mice (n = 9) to the same protocol as in Figure 2, but this time we replaced the prosthesis with a white rectangular block (Figure 3A). In these experiments, we did find that, similar to the artificial limb embodiment, there was a significant difference in average pupil shift in the 2-4 s window after the threat was displayed, both for the right (Wilcoxon test: p = 0.039, Figure 3 B,C) and left pupil (Wilcoxon test: p = 0.027, Figure 3E,F). However, this initial shift lasted for a shorter amount of time, as the differences in average pupil shift in the 4 to 7 s time window right was not significant (Wilcoxon test: p = 0.36 both for the right and left pupils), and was significantly smaller than the difference that we found for the artificial limb, both for the right (Wilcoxon test: p = 0.0078, Figure 3D) and left pupils (Wilcoxon test: p = 0.0039, Figure 3G).

**Reduced pupil dilation during synchronous stimulations**
In addition to the pupil position, we found that the pupil diameter differed between visuo-tactile pairing conditions. When we measured the average pupil diameter 2.5-5.5 s after the application of the threat (Figure 4A-E), we found a significant difference between synchronous and asynchronous stimulations in the artificial limb condition (Wilcoxon test: p = 0.027) but not the in the block condition (Wilcoxon test: p = 0.13, Figure 4B,D). In a second interval (5.5 to 9 s) we found a significant difference between synchronous and asynchronous stimulations, this time regardless of the prosthesis shape (Wilcoxon test prosthesis condition: p= 0.002, white block condition: p= 0.0078, Figure 4B,D).

And when comparing the amount of synchronous/asynchronous difference in pupil diameter between the prosthesis versus white block conditions (Figure 4E), we found that it was significantly more pronounced in the prosthesis condition during the first time interval (Wilcoxon test: p=0. 039) but not the second (Wilcoxon test: p=0.055).

Looking now at the left pupil, we found a similar effect, although significance shifted to the second time interval: on the first time interval, the differences between synchronous and asynchronous stimulations for both prosthesis forms were not significant (Wilcoxon test prosthesis condition: p=0.38, white block condition: p=0.3), while we found a significant differences for the second time interval (Wilcoxon test prosthesis condition: p=0.02, white block condition: p=0. 0039, Figure 4G,I), and a significant difference

between the effect seen with a prosthesis and the one seen with a white block during the second time interval (Wilcoxon test: p=0. 0078) but not the first (Wilcoxon test: p=0.5, Figure 4J).

Overall, we found that both pupils of the mice were less open during the synchronous stimulation of a prosthesis resembling the animal's paw. This effect started earlier and had a higher amplitude in the right pupil which is directly looking at the prosthesis.

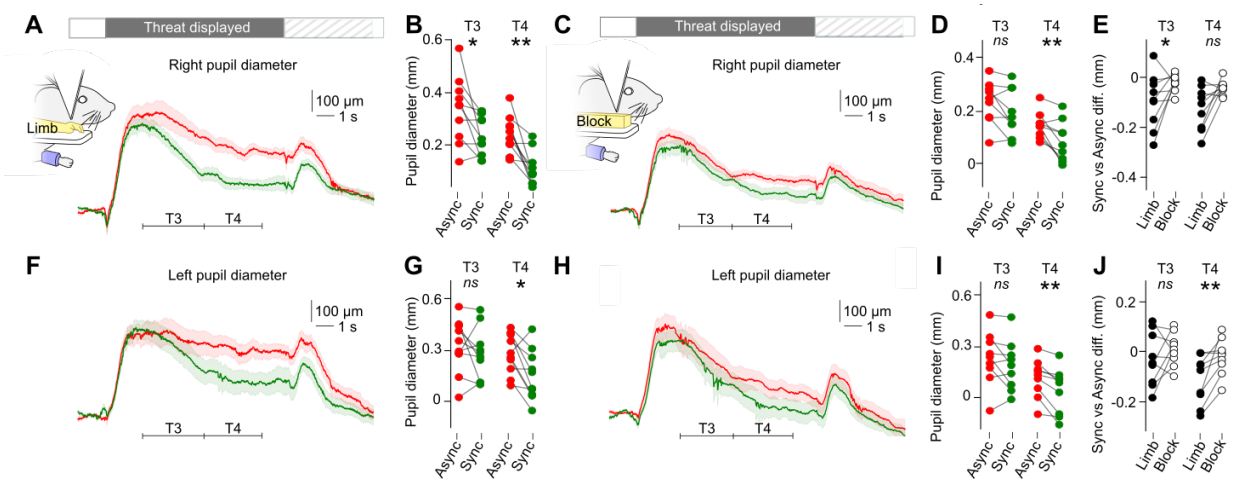


**Figure 4. Pupils are less dilated in response to the threat in the synchronous condition**
(**A**) Average vertical diameter of the right pupil after the threat in the artificial limb condition, normalized relative to the mean position of the second before the threat (n=10). T3 and T4 are the time intervals used for the Wilcoxon test in (B). Light background: SEM.
(**B**) Average of the right pupil diameter for each mouse (n = 9) during the intervals T3 and T4 shown in **A**. *: Wilcoxon p = 0.027, **: Wilcoxon p = 0.002.
(**C**) Variation of the average vertical diameter of the right pupil after the threat in the white block condition, normalized relative to the mean position of the second before the threat (n=9). T3 and T4 are the time intervals used for the Wilcoxon test in (B). Light background: SEM.
(**D**) Normalized average of the right pupil diameter for each mouse (n = 9) during the intervals T3 and T4 shown in **C**. ns: Wilcoxon p = 0.13, **: Wilcoxon p = 0.0078.
(**E**) Difference between the normalized average right pupil diameters between synchronous and asynchronous conditions for the artificial limb condition (black) versus white rectangle condition (white) during intervals T3 and T4. Top: right pupil. Bottom: left pupil. *: Wilcoxon p = 0.039, ns: Wilcoxon p = 0.055.
(**F**,**G**,**H**,**I** and **J**) same as **A**,**B**,**C**,**D** and **E** for the left pupil. **G** ns: Wilcoxon p = 0.38, *: Wilcoxon p = 0.02. **I** ns: Wilcoxon p = 0.3, **: Wilcoxon p = 0.0039. **J** ns: Wilcoxon p = 0.5, **: Wilcoxon p = 0.0078.

**Increased whisking and ear movement speed after the threat of the rubber paw.**
In addition to pupil-related variable, when looking at the average horizontal ear movements speed 0-3 s after the prosthesis threat (Figure 5A-C), we found a significant difference between the synchronous and asynchronous pairing conditions (Wilcoxon p = 0.037), and this difference was not significant in the control condition when we replace the prosthesis with a white block (Wilcoxon p = 0.36, Figure 5C). Note however that, when comparing the amount of the sync/async difference in ear speed between the white block condition, we found no significance (Wilcoxon p = 0.16, Figure 5C).

Similarly, when looking at the horizontal component of the average speed of whisking in a 0-2 s window after the threat onset (Figure 5D-F), we found a difference between synchronous and asynchronous conditions, which was only significant when mice were exposed to the artificial limb (Wilcoxon test: p= 0.049) but not when they were exposed to a control object (Wilcoxon test: p= 0.57, Figure 5E). Again, we saw no differences when directly comparing the prosthesis and white rectangle conditions (Wilcoxon test: p= 0.16, Figure 5F).

Overall, we found indications that the mouse grimace (Langford et al., 2010; Wada et al., 2016) tracking could be part of the indicators of limb embodiment. These makers were however not as prominent as the ones we found when focusing on pupil position and diameter dynamics.

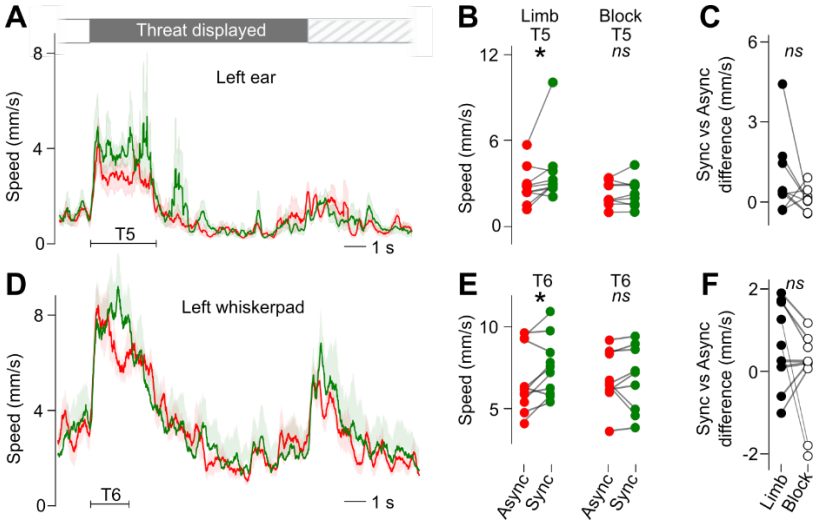


**Figure 5. Increased changes in mice facial grimace after the synchronous stimulation of the prosthesis**
(**A**) Average speed of the left ear after the threat (n=9) smoothed using a 40-element moving average filter via convolution. Light background : SEM
(**B**) Average of ear movement speed for each mouse (n = 9) during interval T4 (see **A**) for the prosthesis (test) and white rectangle (control) conditions. *: Wilcoxon p = 0.037, ns: Wilcoxon p = 0.36.
(**C**) Difference between left ear speed in the synchronous and asynchronous conditions for the artificial limb condition (black) versus white rectangle condition (white) during interval T4. There is no significant difference between the block versus artificial limb contribution to the reaction. ns: Wilcoxon p = 0.16.
(**D**, **E** and **F**) same as **A**, **B** and **C** for the speed of the left whiskerpad movements. **E** *: Wilcoxon p = 0.049, ns: Wilcoxon p = 0.57. **F** ns: Wilcoxon p = 0.16.

# Discussion

### Similarity of the rubber forelimb and rubber hand experimental design

In our experiment we exposed mice to a protocol that was directly derived from the design of the human rubber hand illusion. Our protocol was most similar to the vertical setups of the rubber hand illusion (Kalckert & Ehrsson, 2017). Consistent with these experiments, the artificial forelimb was placed on a platform 1.2 cm on top of the mouse's real paw. In our case, in order to adapt to the mouse anatomy, we also placed the prothesis 0.8 cm away from the mouse horizontally. These distances were the minimum achievable shift to ensure that the prosthesis would be seen by the mouse while remaining at a congruent position anatomically. We stayed in a distance radius of less than 1.5 cm which corresponds in mice to the 30 cm radius where the illusion can still be experienced in human experiments (Lloyd, 2007).

In the classic rubber hand illusion, participants are asked to remain static and focus their attention on the prosthesis (Abdulkarim et al., 2021; Botvinick & Cohen, 1998). To be able to achieve this in mice, we head-fixed the animals and restrained their paw which is a considerable change from the conditions in human experiments. This required habituating the animals to this condition which took around 1 to 2 weeks. This change was important as it allowed us to stimulate the same regions on the paw without any disturbances caused by movement as we know tactile and motor congruency is important for the emergence and maintenance of the illusion (Abdulkarim et al., 2023; Shimada et al., 2009). Our brush stimulations arrived at a frequency ranging between 0.6 and 2 Hz for 2 minutes which is what is usually used is human experiments (Bekrater-Bodmann et al., 2012; Crucianelli et al., 2013; Rohde et al., 2011). Human rubber hand illusion experiments rely mostly on subjective questionnaires to probe the response to the paradigm. However other measures not relying on questionnaires have been developed to measure the strength of the responses. This includes the proprioceptive drift reported in the initial rubber-hand study (Botvinick & Cohen, 1998) where the self-localization of the hand involved in the experiment shifted towards the rubber limb during synchronous conditions. Another alternatives to questionnaires is the bodily response to a threat to the rubber hand: when the rubber limb in embodied in the test conditions, the threatening provokes an anxiety-like response that can be seen cortically as an increased activity in the insula and anterior cingulate cortex (Ehrsson et al., 2007) as well as through skin conductance response (SCR). These responses are also accompanied by participants' reports

indicating an anticipation of pain, as well as facial, verbal and motor signs of surprise or nervousness upon the threat or injury of the fake limb (Armel & Ramachandran, 2003).

With no access to subjective questionnaires in the mouse model, we therefore based our analysis on the detection of a reaction to the threat of a prosthesis, which was already validated in the mouse model in the context of the rubber tail illusion (Wada et al., 2016). In human rubber hand experiments, threats include exhibition of a sharp object like a knife or a needle (Ehrsson et al., 2007). However, their threatening action stems from preestablished cognitive framework recognizing these objects as potentially causing harm which is why we could not use them in rodent experiments. Previous studies investigating this phenomenon in mice used a strong grasp of the tail as a threat (Wada et al., 2016), we wanted our setup to be experimenter independent so our approach is based on a fast-moving object approaching the prosthesis as we found it to be efficient to elicit a strong response in mice while being similar to impact based approaches in human paradigms that elicit SCR responses (Ma & Hommel, 2013).

**Pupil position is a key observable**

In our experiments, the mice showed signs of embodiment that were consistent with the human observation of a difference in the reaction to a menace in synchronous versus asynchronous pairing conditions. In particular, our videography of the mice's face revealed a coupled right and left pupil shifts towards the prosthesis and threat, which lasted longer and was significantly more prominent in the synchronous pairing condition (Figure 2) and very low when only the threat was applied (Figure S1). In two previous studies that investigated tail embodiment in mice through a rubber hand illusion (Wada et al., 2016, 2019), head movements were reported as the reaction of the mice to a menace to the tail. However, in our experiments, the mice were head fixed, and therefore pupil movements were likely used by the mice to rotate their gaze despite the head fixation (Meyer et al., 2020).

**Impact of the shape of the embodied object**

In our experiments, we have asked, if in the mouse model, there was an impact of the rubber limb shape on the observed pupil shifts (Figure 3). Human experiments have explored the limits of artificial limb embodiment by studying the impact of the similarity of an artificial hand to a physiological limb in the rubber hand illusion (Finotti et al., 2023; Tsakiris et al., 2010) and virtual environments (Zhang et al., 2023). These experiments tend to show higher scores of embodiment for hand shaped objects compared to non-limb objects. Zhang et al show that participants in VR environments tend to look less at minimal hands as well. To take into account these findings, we designed our rubber forelimb shape to be faithful to mouse forelimb anatomy (Wang 2015) and we applied to it a C57BL/6 mouse colour scheme, consistent with our mouse line of interest. To test for the specificity of the shape of the object being embodied, we replaced the artificial limb shape by a white rectangular block (Figure 3). We found that in this condition, the differences in pupil shift between synchronous and asynchronous stimulations lasted for a shorter time. Although we did not find a total collapse of the difference between the synchronous and asynchronous conditions, these results suggest that consistent with human results, mice are more capable to embody of a limb-like object rather than an arbitrary shape.

**Contributions to the fluctuations of pupil diameter**

Beyond the position of the pupil, we also found significant differences in the dynamics of the pupil diameter (Figure 4). After the threat of the rubber paw, we observed pupil dilation that can also be observed when only the threat is applied without prior exposition to the prosthesis and tactile stimulations (Figure S1). Pupil dilation has been shown to correlate with different arousal states (Reimer et al., 2014; Turner et al., 2023), attention (Abdolrahmani et al., 2021), as well as the processing of startling stimuli (Leuchs et al., 2019) and fear conditioning (Poli et al., 2023). We interpret this increase in pupil diameter as a sign that mice were strongly engaged by the arrival of the threat in all conditions in a similar manner. Beyond this overall trend, we noticed that the right pupil diameter was significantly larger in the asynchronous condition in a 2.5 s window after the threat following the initial pupil dilation and 5.5 s for the left pupil. The dynamics of pupil size are known to reflect cognitive processes, including memorization. For instance, studies have shown that pupil constriction is stronger when individuals are exposed to images that they later recall (Naber et al., 2013), or when encountering novel stimuli (Kafkas & Montaldi, 2015). Additionally, pupil size adjustments are linked to the rapid switching between rod-driven and cone-driven vision systems, which allows animals to adapt their visual perception to specific environmental cues (Franke et al., 2022; Qiu et al., 2021). These insights may elucidate the delayed reduction in pupil size observed after the initial dilation in our test condition.

**Towards grimace tracking of embodiment**

The tracking of mice's facial expression has become a relevant strategy to probe different emotional states of the animal. When provoking a negative reaction such as fear, studies show that the animals grimace differs significantly from a neutral emotion (Dolensek et al., 2020; Langford et al., 2010), in particular by modulating the ear and whiskerpad areas of the face. Facial tracking techniques (Mathis et al., 2018) allowed us to quantify the reactivity of mice to the menace presented on the prosthesis and compare this reaction across different conditions. Consistent with the main features of previously reported mouse grimaces, we found that beyond the pupil, the ear and whiskerpad moved faster in response to the threat of the prosthesis-like object after synchronous stimulations compared to the asynchronous control although these effects were less prominent than the ones observed for the pupils (Figure 5). Traces of the baseline responses to the threat alone also show that the response is weaker in this condition compared to our test condition where animals moved faster (Figure S1).

**Perspective**

Our work adds to the existing literature on body ownership in rodents and demonstrates behavioral correlates of forelimb embodiment in mice by reproducing key features of the embodiment in the rubber hand experiment context, including the reduction of embodiment following the degradation of the rubber hand shape. These experiments suggest that limb embodiment is shared across multiple mammalian species and could therefore be investigated in the rodent model using a broad array of experimental strategies.

The methodology used in the experiments constitute a non-invasive videography strategy to probe forelimb embodiment in mice. In the future, this assay could be combined with invasive neuronal recordings and brain manipulations to explore the neuronal basis of embodiment and probe novel strategies to induce prosthesis embodiment.

**Bibliography**

Abdolrahmani, M., Lyamzin, D. R., Aoki, R., & Benucci, A. (2021). Attention separates sensory and motor signals in the mouse visual cortex. *Cell Reports*, *36*(2), 109377. https://doi.org/10.1016/j.celrep.2021.109377

Abdulkarim, Z., Guterstam, A., Hayatou, Z., & Ehrsson, H. H. (2023). Neural substrates of body ownership and agency during voluntary movement. *Journal of Neuroscience*. https://doi.org/10.1523/JNEUROSCI.1492-22.2023

Abdulkarim, Z., Hayatou, Z., & Ehrsson, H. H. (2021). Sustained rubber hand illusion after the end of visuotactile stimulation with a similar time course for the reduction of subjective ownership and proprioceptive drift. *Experimental Brain Research*, *239*(12), 3471–3486. https://doi.org/10.1007/s00221-021-06211-8

Armel, K. C., & Ramachandran, V. S. (2003). Projecting sensations to external objects: Evidence from skin conductance response. *Proceedings of the Royal Society of London. Series B: Biological Sciences*, *270*(1523), 1499–1506. https://doi.org/10.1098/rspb.2003.2364

Bekrater-Bodmann, R., Foell, J., Diers, M., & Flor, H. (2012). The perceptual and neuronal stability of the rubber hand illusion across contexts and over time. *Brain Research*, *1452*, 130–139. https://doi.org/10.1016/j.brainres.2012.03.001

Bekrater-Bodmann, R., Reinhard, I., Diers, M., Fuchs, X., & Flor, H. (2021). Relationship of prosthesis ownership and phantom limb pain: Results of a survey in 2383 limb amputees. *Pain*, *162*(2), 630–640. https://doi.org/10.1097/j.pain.0000000000002063

Botvinick, M., & Cohen, J. (1998). Rubber hands 'feel' touch that eyes see. *Nature*, *391*(6669), Article 6669. https://doi.org/10.1038/35784

Castro, F., Lenggenhager, B., Zeller, D., Pellegrino, G., D'Alonzo, M., & Di Pino, G. (2023). From rubber hands to neuroprosthetics: Neural correlates of embodiment. *Neuroscience & Biobehavioral Reviews*, *153*, 105351. https://doi.org/10.1016/j.neubiorev.2023.105351

Crucianelli, L., Metcalf, N. K., Fotopoulou, A. (Katerina), & Jenkinson, P. M. (2013). Bodily pleasure matters: Velocity of touch modulates body ownership during the rubber hand illusion. *Frontiers in Psychology*, *4*. https://doi.org/10.3389/fpsyg.2013.00703

Dolensek, N., Gehrlach, D. A., Klein, A. S., & Gogolla, N. (2020). Facial expressions of emotion states and their neuronal correlates in mice. *Science (New York, N.Y.)*, *368*(6486), 89–94. https://doi.org/10.1126/science.aaz9468

Ehrsson, H. H., Rosén, B., Stockselius, A., Ragnö, C., Köhler, P., & Lundborg, G. (2008). Upper limb amputees can be induced to experience a rubber hand as their own. *Brain*, *131*(12), 3443–3452. https://doi.org/10.1093/brain/awn297

Ehrsson, H. H., Spence, C., & Passingham, R. E. (2004). That's My Hand! Activity in Premotor Cortex Reflects Feeling of Ownership of a Limb. *Science*, *305*(5685), 875–877. https://doi.org/10.1126/science.1097011

Ehrsson, H. H., Wiech, K., Weiskopf, N., Dolan, R. J., & Passingham, R. E. (2007). Threatening a rubber hand that you feel is yours elicits a cortical anxiety response. *Proceedings of the National Academy of Sciences*, *104*(23), 9828–9833. https://doi.org/10.1073/pnas.0610011104

Espinosa, M., & Nathan-Roberts, D. (2019). Understanding Prosthetic Abandonment. *Proceedings of the Human Factors and Ergonomics Society Annual Meeting*, *63*(1), 1644–1648. https://doi.org/10.1177/1071181319631508

Feinberg, T. E., Venneri, A., Simone, A. M., Fan, Y., & Northoff, G. (2010). The neuroanatomy of asomatognosia and somatoparaphrenia. *Journal of Neurology, Neurosurgery, and Psychiatry*, *81*(3), 276–281. https://doi.org/10.1136/jnnp.2009.188946

Finotti, G., Garofalo, S., Costantini, M., & Proffitt, D. R. (2023). Temporal dynamics of the Rubber Hand Illusion. *Scientific Reports*, *13*(1), 7526. https://doi.org/10.1038/s41598-023-33747-2

Franke, K., Willeke, K. F., Ponder, K., Galdamez, M., Zhou, N., Muhammad, T., Patel, S., Froudarakis, E., Reimer, J., Sinz, F. H., & Tolias, A. S. (2022). State-dependent pupil dilation rapidly shifts visual feature selectivity. *Nature*, *610*(7930), 128–134. https://doi.org/10.1038/s41586-022-05270-3

Kalckert, A., & Ehrsson, H. H. (2017). The Onset Time of the Ownership Sensation in the Moving Rubber Hand Illusion. *Frontiers in Psychology*, *8*. https://doi.org/10.3389/fpsyg.2017.00344

Langford, D. J., Bailey, A. L., Chanda, M. L., Clarke, S. E., Drummond, T. E., Echols, S., Glick, S., Ingrao, J., Klassen-Ross, T., LaCroix-Fralish, M. L., Matsumiya, L., Sorge, R. E., Sotocinal, S. G., Tabaka, J. M., Wong, D., van den Maagdenberg, A. M. J. M., Ferrari, M. D., Craig, K. D., & Mogil, J. S. (2010). Coding of facial expressions of pain in the laboratory mouse. *Nature Methods*, *7*(6), Article 6. https://doi.org/10.1038/nmeth.1455

Leuchs, L., Schneider, M., & Spoormaker, V. I. (2019). Measuring the conditioned response: A comparison of pupillometry, skin conductance, and startle electromyography. *Psychophysiology*, *56*(1), e13283. https://doi.org/10.1111/psyp.13283

Lloyd, D. M. (2007). Spatial limits on referred touch to an alien limb may reflect boundaries of visuo-tactile peripersonal space surrounding the hand. *Brain and Cognition*, *64*(1), 104–109. https://doi.org/10.1016/j.bandc.2006.09.013

Ma, K., & Hommel, B. (2013). The virtual-hand illusion: Effects of impact and threat on perceived ownership and affective resonance. *Frontiers in Psychology*, *4*. https://doi.org/10.3389/fpsyg.2013.00604

Maimon-Mor, R. O., & Makin, T. R. (2020). Is an artificial limb embodied as a hand? Brain decoding in prosthetic limb users. *PLOS Biology*, *18*(6), e3000729. https://doi.org/10.1371/journal.pbio.3000729

Mathis, A., Mamidanna, P., Cury, K. M., Abe, T., Murthy, V. N., Mathis, M. W., & Bethge, M. (2018). DeepLabCut: Markerless pose estimation of user-defined body parts with deep learning. *Nature Neuroscience*, *21*(9), Article 9. https://doi.org/10.1038/s41593-018-0209-y

Meyer, A. F., O'Keefe, J., & Poort, J. (2020). Two Distinct Types of Eye-Head Coupling in Freely Moving Mice. *Current Biology*, *30*(11), 2116-2130.e6. https://doi.org/10.1016/j.cub.2020.04.042

Poli, A., Viglione, A., Mazziotti, R., Totaro, V., Morea, S., Melani, R., Silingardi, D., Putignano, E., Berardi, N., & Pizzorusso, T. (2023). Selective Disruption of Perineuronal Nets in Mice Lacking Crtl1 is Sufficient to Make Fear Memories Susceptible to Erasure. *Molecular Neurobiology*, *60*, 1–15. https://doi.org/10.1007/s12035-023-03314-x

Qiu, Y., Zhao, Z., Klindt, D., Kautzky, M., Szatko, K. P., Schaeffel, F., Rifai, K., Franke, K., Busse, L., & Euler, T. (2021). Natural environment statistics in the upper and lower visual field are reflected in mouse retinal specializations. *Current Biology*, *31*(15), 3233-3247.e6. https://doi.org/10.1016/j.cub.2021.05.017

Reader, A. T., Trifonova, V. S., & Ehrsson, H. H. (2021). The Relationship Between Referral of Touch and the Feeling of Ownership in the Rubber Hand Illusion. *Frontiers in Psychology*, *12*. https://doi.org/10.3389/fpsyg.2021.629590

Reimer, J., Froudarakis, E., Cadwell, C. R., Yatsenko, D., Denfield, G. H., & Tolias, A. S. (2014). Pupil Fluctuations Track Fast Switching of Cortical States during Quiet Wakefulness. *Neuron*, *84*(2), 355–362. https://doi.org/10.1016/j.neuron.2014.09.033

Rohde, M., Luca, M. D., & Ernst, M. O. (2011). The Rubber Hand Illusion: Feeling of Ownership and Proprioceptive Drift Do Not Go Hand in Hand. *PLOS ONE*, *6*(6), e21659. https://doi.org/10.1371/journal.pone.0021659

Rosén, B., Ehrsson, H. H., Antfolk, C., Cipriani, C., Sebelius, F., & Lundborg, G. (2009). Referral of sensation to an advanced humanoid robotic hand prosthesis. *Scandinavian Journal of Plastic and Reconstructive Surgery and Hand Surgery*, *43*(5), 260–266. https://doi.org/10.3109/02844310903113107

Salay, L. D., Ishiko, N., & Huberman, A. D. (2018). A midline thalamic circuit determines reactions to visual threat. *Nature*, *557*(7704), Article 7704. https://doi.org/10.1038/s41586-018-0078-2

Shimada, S., Fukuda, K., & Hiraki, K. (2009). Rubber Hand Illusion under Delayed Visual Feedback. *PLOS ONE*, *4*(7), e6185. https://doi.org/10.1371/journal.pone.0006185

Tsakiris, M., Carpenter, L., James, D., & Fotopoulou, A. (2010). Hands only illusion: Multisensory integration elicits sense of ownership for body parts but not for non-corporeal objects. *Experimental Brain Research*, *204*(3), 343–352. https://doi.org/10.1007/s00221-009-2039-3

Turner, K. L., Gheres, K. W., & Drew, P. J. (2023). Relating Pupil Diameter and Blinking to Cortical Activity and Hemodynamics across Arousal States. *Journal of Neuroscience*, *43*(6), 949–964. https://doi.org/10.1523/JNEUROSCI.1244-22.2022

Vinck, M., Batista-Brito, R., Knoblich, U., & Cardin, J. A. (2015). Arousal and Locomotion Make Distinct Contributions to Cortical Activity Patterns and Visual Encoding. *Neuron*, *86*(3), 740–754. https://doi.org/10.1016/j.neuron.2015.03.028

Wada, M., Ide, M., Atsumi, T., Sano, Y., Shinoda, Y., Furuichi, T., & Kansaku, K. (2019). Rubber tail illusion is weakened in Ca2+-dependent activator protein for secretion 2 (Caps2)-knockout mice. *Scientific Reports*, *9*(1), Article 1. https://doi.org/10.1038/s41598-019-43996-9

Wada, M., Takano, K., Ora, H., Ide, M., & Kansaku, K. (2016). The Rubber Tail Illusion as Evidence of Body Ownership in Mice. *Journal of Neuroscience*, *36*(43), 11133–11137. https://doi.org/10.1523/JNEUROSCI.3006-15.2016

Zhang, J., Huang, M., Yang, R., Wang, Y., Tang, X., Han, J., & Liang, H.-N. (2023). Understanding the effects of hand design on embodiment in virtual reality. *AI EDAM*, *37*, e10. https://doi.org/10.1017/S0890060423000045

## Supplementary Material :

| | | Session 1 | Session 2 | Session 3 | Session 4 | Session 5 |
|---|---|---|---|---|---|---|
| Prosthesis | Group A (19,21,23,25,27) | Synchronous<br>Asynchronous | Asynchronous<br>Synchronous | Synchronous<br>Asynchronous | Asynchronous<br>Synchronous | Synchronous<br>Asynchronous |
| | Group B (20,22,24,26,28) | Asynchronous<br>Synchronous | Synchronous<br>Asynchronous | Asynchronous<br>Synchronous | Synchronous<br>Asynchronous | Asynchronous<br>Synchronous |
| White and block threat only | Group A (19,21,23,25,27 | Threat Only<br>Synchronous<br>Asynchronous | Threat Only<br>Asynchronous<br>Synchronous | Threat Only<br>Synchronous<br>Asynchronous | Threat Only<br>Asynchronous<br>Synchronous | Threat Only<br>Synchronous<br>Asynchronous |
| | Group B (22,24,26,28) | Threat Only<br>Asynchronous<br>Synchronous | Threat Only<br>Synchronous<br>Asynchronous | Threat Only<br>Asynchronous<br>Synchronous | Threat Only<br>Synchronous<br>Asynchronous | Threat Only<br>Asynchronous<br>Synchronous |

**Table 1. Trial Order for experimental paradigm.**

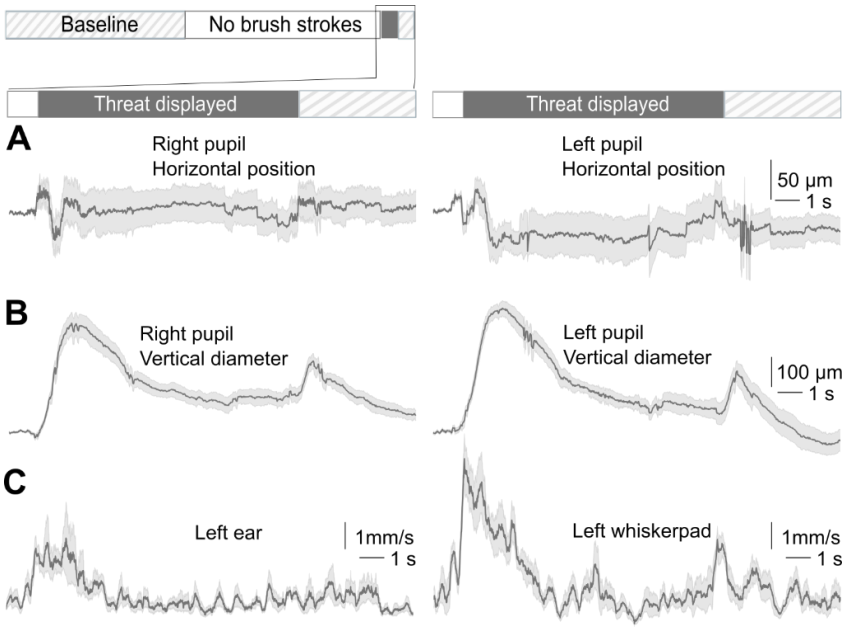


**Figure S1. Baseline responses to the threat presented alone without the prosthesis and brush strokes.**
In the threat only condition, the animals are not exposed to the prosthesis nor the stimulations. An empty platform identical to the platform that usually holds the prosthesis is placed next to them at the same position.
(**A**) Average horizontal position of the right and left pupil after the threat, normalized relative to the mean position of the second before the threat (n=9). Light background: SEM.
(**B**) Average vertical diameter of the right and left pupil after the threat, normalized relative to the mean position of the second before the threat (n=9). Light background: SEM.
(**C**) Average speed of the left ear and left whisker pad after the threat (n=9) smoothed using a 40-element moving average filter via convolution. Light background: SEM.